Lens Based Switched Beam Antenna for a 5G Smart Repeater

Jordi Romeu, *Fellow , IEEE*, Sebastián Blanch, Lluís Pradell, *Life Member, IEEE*, Antoni Barlabé, *Member, IEEE*, Juan-Manuel Rius, *Senior Member, IEEE*, Miquel Albert-Gali, Lluís Jofre-Roca, *Life Fellow, IEEE*, Christian Mazzucco *Member, IEEE,* and Roberto Flamini, *Member, IEEE,*

***Abstract*—A 16 switched beam lens based antenna with a coverage area of $\pm 30^{\circ}$ in the horizontal plane and from 0 to -20° in the vertical plane has been built and tested. The intended use of the antenna is as part of a smart repeater servicing the coverage area of a 5G wireless communication system operating in the n258 band of the 5G Frequency Range 2, from 24.25 to 27.5 GHz. The antenna has been built using state-of-the-art materials and components in order to assess the performance of this antenna concept. The overall antenna losses including the feeding network are of the order of 8 dB and the realized gain in the 80% of the coverage area is above 11 dB.**

***Index Terms*—lens antenna, network conrolled repeater, switched beam, 5G, FR2**

I. Introduction

THE deployment of 5G New Radio (NR) mobile networks operating at the mmWave frequency spectrum poses specific challenges in order to achieve a proper coverage level in complex propagation environments. The move towards the use of higher frequencies results in larger free space propagation losses and greater blocking effects produced by obstacles such as buildings, foliage and body [1]. As discussed in [2] a way to overcome this shortfall is the use of Smart Repeaters, also called NR Network-Controlled Repeaters (NCR) [3]. A Network-controlled repeater is an in-band RF repeater used for extension of network coverage and it can be considered as an evolution of a conventional RF repeater since it has the capability to receive and process side control information from the network. The most important features of a Network-controlled repeater are the following: i) mitigation of unnecessary noise amplification by means of Power control and ON/OFF control, ii) beamforming capability to perform transmissions and receptions with better spatial directivity, iii) UpLink (UL) -DownLink (DL) TDD (Time Division Duplex) configuration. A NCR is a system composed by two antennas one oriented to the base station (or gNB as it is called in 5G NR terminology) and the other oriented towards the service area to be covered, and an amplification chain in between. The NCR receives a signal in DL (or UL) by the first antenna, performs a power (analog only) amplification and, with a proper beamforming, it forwards the signal in DL (or UL). In its simplest form the repeater has to be low cost, easy to deploy and non-regenerative as they do not decode and re-code the input signal. While the antenna pointing towards the donor gNB can be a single-beam antenna pointing towards the gNB, the one servicing the coverage area has to be a multiple beam reconfigurable antenna. The reason it that the key performance indicator of the NCR is the Equivalent Isotropic Radiated Power (EIRP) in the service area. The way to increase the EIRP is the use of antennas with high gain and narrow beam that are pointed towards the user in the service area. In addition by using narrow beams interference and mutual coupling is reduced.

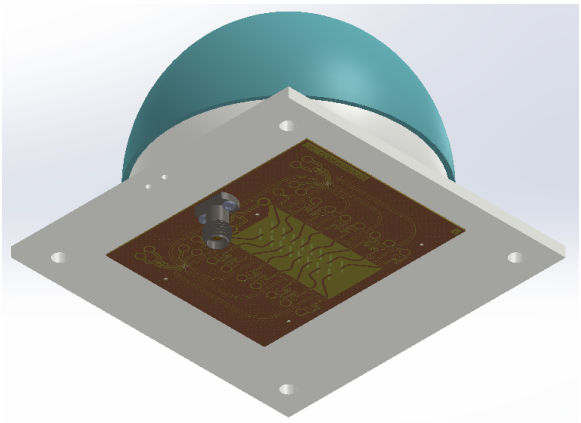

Fig. 1. Geometry of lens based switched beam antenna. In white the lens made of a dielectric material with $\epsilon_r = 5$, blue the 3D-printed matching layer and the RF circuitry is glued on the lens base.

One way to achieve narrow beams tracking the user location is by using phased arrays [4],[5], but solutions based on switching diodes can be advantageous for low cost applications. For example, beam pointing can be achieved by inserting switching PIN diodes in a metasurface antenna [6]. Also, a five-beam switched antenna at 28 GHz can be made by PIN diodes short-circuiting slots on a waveguide [7]. In this paper a lens based switched beam antenna with 16 beams for the n258 band of the 5G Frequency Range 2, from 24.25 to 27.5 GHz is proposed. The use of lens based switched beam antennas for millimeter wave frequency communications has been previously suggested [8],[9],[10],[11], and here we present

Manuscript received xxxx, 2023. This work was funded in part by AEI: PID2019-107885GB-C31/AEI/10.13039/501100011033 and HUAWEI TECHNOLOGIES Italia S.r.l

J. Romeu, S. Blanch, L. Pradell, A. Barlabé, J-M Rius, M. Albert-Galí and L. Jofre-Roca are with Universitat Politecnica de Catalunya, Barcelona, 08034 Spain. (e-mail: jordi.romeu-robert@upc.edu)

C. Mazzucco and R. Flamini are with the Milan Research Center of Huawei Technologies Italia S.r.l, Milan, Italy, (e-mail: roberto.flamini@huawei.com).

a working prototype built with state-of-the-art materials and components. This full working prototype allows to compare this technological option in front other solutions in terms of performance, complexity and bill of materials.

Opting for the switched beam lens antenna is done for the sake of a much simpler RF architecture in terms of number of radiating elements, distribution network and RF electronics, and the consequent cost reduction. The antenna specification is to scan $\pm 30°$ in the horizontal plane and $0°$ to $-20°$ in the vertical plane with fixed $45°$ linear polarization with 8×2 beams. The radiation pattern is aimed at increasing the coverage in dense urban areas [2]. With this specification the beam width of each beam is of the order of $8°$ in each plane in order to have beam overlapping in the coverage area. In order to compare the RF architecture of the proposed solution with an equivalent phased array it is interesting to estimate the number radiating elements that a phased array with similar beam scanning would require. Notice that to achieve the required beam width a square aperture of approximately $6.5\lambda_0$ side length is required, where λ_0 is the free space wavelength. In order to avoid grating lobes when the beam is scanned, array element spacing should be smaller than $0.7\lambda_0$ which would lead to an array of about $10 \times 10 = 100$ elements with the corresponding RF feeding network and phase shifting electronics. In Section II the antenna requirements, the proposed solution and its working principle are presented. In Section III the measured results of the antenna are presented. Finally, the conclusions are discussed in Section IV.

II. Antenna Description

In the proposed solution beam scan is achieved by switching between 16 radiating elements placed on the focal plane of a lens. Thus the antenna is formed by the lens, the 16 feeding elements properly located on the lens focal plane, and a 1 to 16 switching network. As shown in fig. 1 the RF circuit is glued on the base of the lens. A quarter-wave length matching layer is included in the design.

A. Lens design

The chosen lens geometry is an elliptical dielectric lens [12], where the choices to be made are the relative dielectric constant of the lens ϵ_r , and the lens minor axis a, the rest of parameters are found as (Fig. 2):

$$b = \frac{a}{\sqrt{1 - \frac{1}{\epsilon_r}}}; L = \frac{b}{\sqrt{\epsilon_r}}$$
$$x = a\cos(\alpha); y = L + b\sin(\alpha) \quad (1)$$

The advantage of employing an elliptical lens is that it requires only one homogeneous material. Other alternatives such as Luneburg lenses require the use of shells of different materials or to produce a Graded Refraction Index material [13] The lens minor axis a sets the lens diameter and is determined by the required radiation pattern beam width. As a starting point it can be assumed that $\Delta\theta = \frac{2a}{\lambda_0}$, that with the required beam width of approximately $8°$ leads to a lens diameter $2a$ of the order of 80 mm. From (1) increasing ϵ_r reduces the dimension of the major axis b and results in a more compact lens. Nevertheless, it must be noted that as pointed in [14] for a given displacement of the feed in the focal plane, the beam tilting increases as the lens dielectric constant ϵ_r increases. This behavior implies that in order to produce overlapping beams the feeding elements have to be closer as the value of ϵ_r increases. In consequence high dielectric constant lenses may lead to very close feeding elements to produce overlapping beams that are unfeasible in practice.

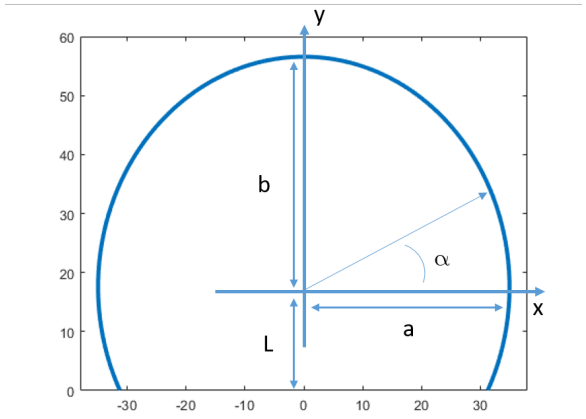

Fig. 2. Geometry of an elliptical dielectric lens.

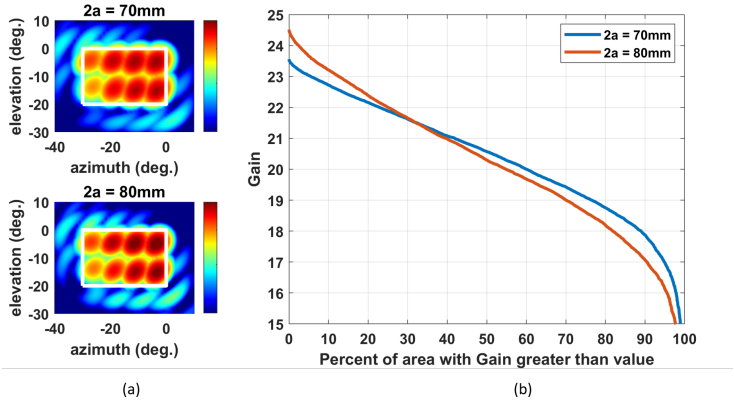

Fig. 3. (a) Simulated antenna beams for a 70 mm lens (top) and a 80 mm lens (bottom). (b) Antenna gain cumulative distribution. Frequency 25.875 GHz.

To build the lens the PREPERM 550 dielectric material from AVIENT with a relative dielectric constant of 5 has been chosen. This value of dielectric constant is a good compromise between lens compactness and feed element spacing. In order to determine the optimum lens antenna diameter, the following trade-off has to be considered. Increasing the lens diameter increases the beams peak gain, but also reduces the beam width and in consequence beam overlapping between beams occurs at a lower gain level. In order to compare the performance of different lens diameters the antenna gain cumulative distribution has been computed. In order to do so, first the combined switched beam antenna pattern is computed

by considering in each direction the maximum gain produced by any beam. Once the combined radiation pattern is found the cumulative gain distribution is obtained by finding the gain that is exceeded with a certain probability within the specified antenna coverage area. In order to determine the feed position that causes the desired beam scan the ILASH software [15] has been used. Once optimum placement of the lens feeds has been determined, full wave simulation of a slot fed lens has been conducted using CST Studio Design. In the simulations a lossless dielectric material has been considered for the lens and matching layer made of quarter-wavelength shell has been included. Notice that the ratio of radiated powers in air and dielectric for an elementary slot is $\epsilon^{3/2}$ [12]. Therefore, for the lens with relative dielectric constant of 5 only a small fraction of the radiated power by slot is not radiated into the lens. Figure 3 (a) shows the resulting combined pattern for a lens of 70 and 80 mm of diameter, where the white rectangle shows the desired coverage area. Due to the symmetry only 8 beams corresponding to the $-30°$ to $0°$ horizontal scan range are shown. From the combined radiation patterns the cumulative gain distribution is found and it is shown in fig. 3 (b). As expected the 80 mm lens produces higher gain beams, but when the exceeded gain in 90% of the coverage area is considered it is observed that the 70 mm lens produces a gain value that is about 1 dB higher than the 80 mm lens, and also a more uniform gain distribution over the coverage area. Additional simulations showed that reducing the lens diameter reduces the antenna peak gain, but does not significantly increase the exceeded gain in 90% of the coverage area, consequently the 70 mm lens has been chosen. In order to estimate the lens losses a slot center fed lens antenna was built and its gain pattern measured. The measured beam width was $8.3°$ and it was estimated that the loss tangent of the PREPERM 550 material at 25.875 GHz is 0.00314, with the corresponding losses of 1.8 dB

B. Feeding network

The distribution network is designed to route the signal to the selected radiating element. To easily integrate the RF circuitry with the radiating element and the lens, a slot etched on the ground plane fed by a short-circuited microstrip line has been used as a feed element. The slot is rotated $45°$ to radiate in the desired polarization. The feeding microstrip line is terminated in short circuit as it results in a smaller dimensions of the feed element. The microstrip substrate is a low loss RO3003 with a thickness 0.25 mm. As shown in figure 4 the RF switching circuitry has a tree structure in which integrated switches and diode-based switches are combined. The reason is to keep a balance between cost, complexity, space usage and finally the interest in testing both approaches. In addition the power handling capability by the integrated switches (1 dB compression point of 27 dBm) is higher than the diodes (maximum incident power 23 dBm), and therefore placing the integrated switches in the first stages of the distribution circuit increases the power radiating capabilities of the antenna. From the antenna input port a SPDT switch based on the ADRF5024 by Analog Devices allows to select the

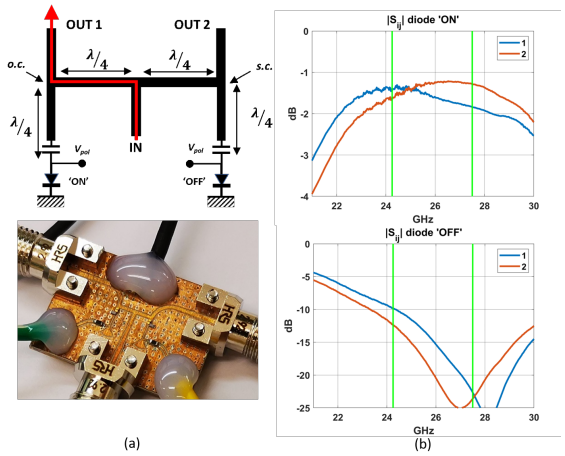

Fig. 4. RF 1 to 16 distribution network showing the location of the switches. The radiating slots are edged on the bottom ground plane. Due to the circuit symmetry only the upper half is shown. The white line shows the RF path followed to feed one of the slots.

upper or lower row of the radiating element. An ADRF5046 SP4T switch in combination of diode-based SPDT allows to select the radiating slot. The diodes used in the SPDT are the MACOM MA4AGFCP910. The diode impedance has been characterized in its ON and OFF state using a CPW set-up. The 50Ω measured normalized impedance for the diode is $0.128 + j0.918$ in the ON state and $0.152 - j1.618$ in the OFF state at 25.875 GHz. The diode presents a low resistance in both states and the impedance phase difference between states is close to $180\,\mathrm{deg}$ which are the necessary requirements to design a low-loss high-isolation SPDT. The diode-based switch is shown in Figure 5. Notice that the exact line lengths have been tuned using Keysight ADS taking into account the measured diode impedance. The results of figure 5 show that including connectors and transmission line losses the insertion losses of the SPDT are below 2 dB. The microstrip path length from the input port to the closest and the furthest slot antenna is 53.7 mm and 88.1 mm respectively. At the lower and upper part of the frequency band of interest the estimated insertion loss with Keysight ADS is 1.24 dB and 1.8 dB for the closest antenna, and 1.69 dB and 2.4 dB for the furthest one. The insertion losses of the ADRF5024 and ADRF5046 according to the manufacturer data sheet measured close to the input and output pins are 1.2 dB and 1.5 dB respectively and input 1 dB compression point of 27 dBm. When the losses of the microstrip transmission lines are considered 6 dB losses in the distribution network are expected.

III. Results

The lens has been milled from a PREPERM PPE500 block and the matching layer has been $3D$ printed. The RF circuit has been glued to the lens. As shown in figure 6 the antenna has been placed in an anechoic chamber to measure the antenna realized gain. In order to assess the return losses without the effect of the switches and the transmission lines, a single slot lens antenna was tested and the measured return losses were better than 10 dB in the frequency band.

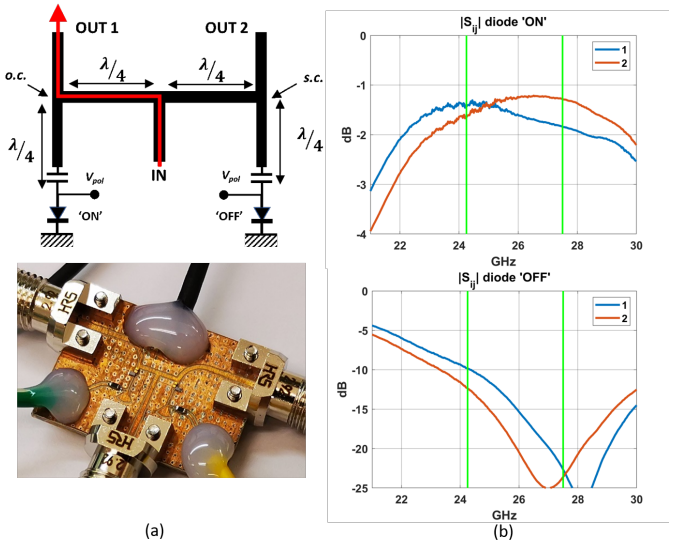

Fig. 5. (a) Circuit layout and implementation of the diode based SPDT. (b) Measured S-parameters for the diode based SPDT switch.

Figure 7 (a) shows the combined radiation pattern for the switched beam antenna. The 16 beam combined radiation pattern covers the specified area. In figure 7 (b) the simulated and measured antenna gain cumulative gain distribution are shown. In the simulation a lossless case has been considered, while in the measurement the losses of the distribution network as well as the losses in the lens are taken into account. It observed that the cumulative gain distribution in simulation and measurement follows a similar pattern with about 8 dB offset due to the antenna losses. In 80% of the coverage area at the center frequency the realized gain of the switched beam antenna is above 11 dB. Considering the power handling of the antenna switches, the antenna should be able to accept an input power of 25 dBm and achieving an EIRP of 36 dBm in 80% of the coverage area.

The losses in the antenna are distributed in the lens dielectric (1.8 dB), microstrip line losses (around 1.5 dB), and the rest (4.7 dB) are lost in the switching devices. The reduction of this latter device dependent losses are beyond the possibilities of the antenna designer. Transmission line losses can be reduced by using structures with smaller losses such as the inverted microstrip gap waveguide [16]. Analogously lens losses can be reduced by using dielectrics with smaller loss tangent. In general lower dielectric constant plastics present lower loss tangent. In [17] measured results for the dielectric constant for different plastics are presented. For instance polypropylene has $\epsilon_r = 2.25$ and $tan\delta = 0.00041$ at 25 GHz. As mentioned earlier, lower dielectric constant lens result in bulkier lenses for a given diameter.

IV. Conclusion

The prototype antenna provided an opportunity to evaluate the performance of the proposed switched-beam lens antenna as a NCR. Given the antenna coverage requirements, this approach results in a simplified RF structure in which the number of required RF components is reduced compared to alternative solutions such as phased arrays. The antenna performance is according to the requirements in terms of area coverage and number of beams. On the other hand, factors contributing to the antenna losses have been identified and potential solutions have been proposed. There are three contributions to the antenna losses: i) losses in the switching devices, ii) losses in the transmission lines and iii) losses in the lens. It is possible to reduce the antenna losses significantly by using plastics with lower dielectric constant and loss tangent in the lens construction, and using alternative transmission lines in the distribution circuitry.

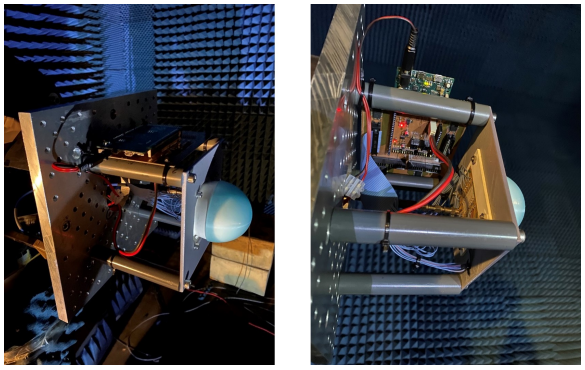

Fig. 6. Switched beam lens antenna placed on the anechoic chamber for radiation pattern measurement.

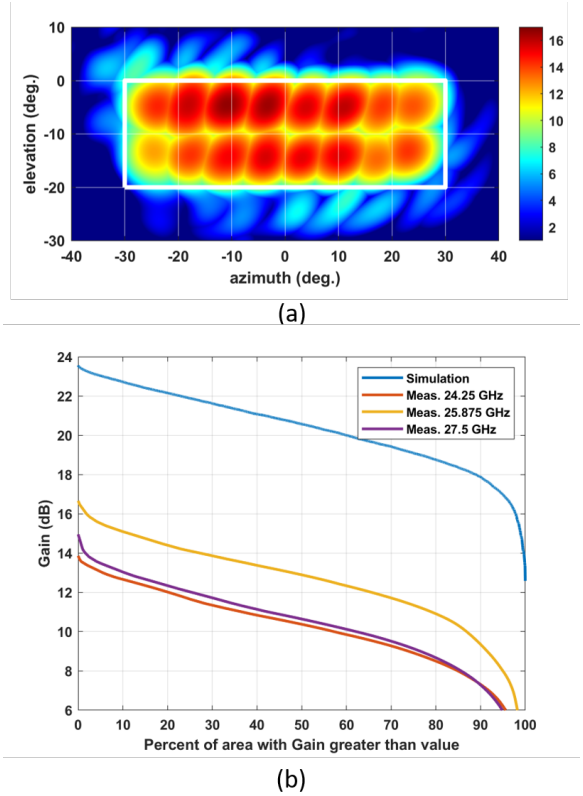

Fig. 7. (a) Measured realized gain patterns for the switched beam lens antenna at the center frequency of 25.875 GHz.(b) Simulated (lossless case) and measured antenna gain cumulative distribution.

REFERENCES

[1] M. Shafi, J. Zhang, H. Tataria, A. F. Molisch, S. Sun, T. S. Rappaport, F. Tufvesson, S. Wu, and K. Kitao, "Microwave vs. millimeter-wave propagation channels: Key differences and impact on 5g cellular systems," *IEEE Communications Magazine*, vol. 56, no. 12, pp. 14–20, 2018.

[2] R. Flamini, D. De Donno, J. Gambini, F. Giuppi, C. Mazzucco, A. Milani, and L. Resteghini, "Toward a heterogeneous smart electromagnetic environment for millimeter-wave communications: An industrial viewpoint," *IEEE Transactions on Antennas and Propagation*, vol. 70, no. 10, pp. 8898–8910, 2022.

[3] 3GPP, "Study on nr network-controlled repeaters," *3GPP TR 38.867*, vol. Release 18, October 2022.

[4] M. Ide, A. Shirane, K. Yanagisawa, D. You, J. Pang, and K. Okada, "A 28-ghz phased-array relay transceiver for 5g network using vector-summing backscatter with 24-ghz wireless power and lo transfer," *IEEE Journal of Solid-State Circuits*, vol. 57, no. 4, pp. 1211–1223, 2022.

[5] A. Bagheri, H. Karlsson, C. Bencivenni, M. Gustafsson, T. Emanuelsson, M. Hasselblad, and A. A. Glazunov, "A 16 × 16 45° slant-polarized gap-waveguide phased array with 65-dbm eirp at 28 ghz," *IEEE Transactions on Antennas and Propagation*, vol. 71, no. 2, pp. 1319–1329, 2023.

[6] E. Martini and S. Maci, "Theory, analysis, and design of metasurfaces for smart radio environments," *Proceedings of the IEEE*, vol. 110, no. 9, pp. 1227–1243, 2022.

[7] Y. Yashchyshyn, K. Derzakowski, G. Bogdan, K. Godziszewski, D. Nyzovets, C. H. Kim, and B. Park, "28 ghz switched-beam antenna based on s-pin diodes for 5g mobile communications," *IEEE Antennas and Wireless Propagation Letters*, vol. 17, no. 2, pp. 225–228, 2018.

[8] M. Imbert, J. Romeu, M. Baquero-Escudero, M.-T. Martinez-Ingles, J.-M. Molina-Garcia-Pardo, and L. Jofre, "Assessment of ltcc-based dielectric flat lens antennas and switched-beam arrays for future 5g millimeter-wave communication systems," *IEEE Transactions on Antennas and Propagation*, vol. 65, no. 12, pp. 6453–6473, 2017.

[9] A. Artemenko, A. Mozharovskiy, A. Maltsev, R. Maslennikov, A. Sevastyanov, and V. Ssorin, "Experimental characterization of e-band two-dimensional electronically beam-steerable integrated lens antennas," *IEEE Antennas and Wireless Propagation Letters*, vol. 12, pp. 1188–1191, 2013.

[10] A. E. Olk and D. A. Powell, "Huygens metasurface lens for w-band switched beam antenna applications," *IEEE Open Journal of Antennas and Propagation*, vol. 1, pp. 290–299, 2020.

[11] F. Foglia Manzillo, M. Śmierzchalski, L. Le Coq, M. Ettorre, J. Aurinsalo, K. T. Kautio, M. S. Lahti, A. E. I. Lamminen, J. Säily, and R. Sauleau, "A wide-angle scanning switched-beam antenna system in ltcc technology with high beam crossing levels for v-band communications," *IEEE Transactions on Antennas and Propagation*, vol. 67, no. 1, pp. 541–553, 2019.

[12] D. Filipovic, S. Gearhart, and G. Rebeiz, "Double-slot antennas on extended hemispherical and elliptical silicon dielectric lenses," *IEEE Transactions on Microwave Theory and Techniques*, vol. 41, no. 10, pp. 1738–1749, 1993.

[13] Z. Larimore, S. Jensen, A. Good, A. Lu, J. Suarez, and M. Mirotznik, "Additive manufacturing of luneburg lens antennas using space-filling curves and fused filament fabrication," *IEEE Transactions on Antennas and Propagation*, vol. 66, no. 6, pp. 2818–2827, 2018.

[14] D. Filipovic, G. Gauthier, S. Raman, and G. Rebeiz, "Off-axis properties of silicon and quartz dielectric lens antennas," *IEEE Transactions on Antennas and Propagation*, vol. 45, no. 5, pp. 760–766, 1997.

[15] E. Lima, J. R. Costa, M. G. Silveirinha, and C. A. Fernandes, "Ilash - software tool for the design of integrated lens antennas," in *2008 IEEE Antennas and Propagation Society International Symposium*, 2008, pp. 1–4.

[16] E. Pucci, A. U. Zaman, E. Rajo-Iglesias, and P.-S. Kildal, "New low loss inverted microstrip line using gap waveguide technology for slot antenna applications," in *Proceedings of the 5th European Conference on Antennas and Propagation (EUCAP)*, 2011, pp. 979–982.

[17] B. Salski, J. Cuper, T. Karpisz, P. Kopyt, and J. Krupka, "Complex permittivity of common dielectrics in 20–110 ghz frequency range measured with a fabry–pérot open resonator," *Applied Physics Letters*, vol. 119, no. 5, p. 052902, 2021. [Online]. Available: https://doi.org/10.1063/5.0054904